
Learning Graph Models for Template-Free Retrosynthesis

Vignesh Ram Somnath¹Charlotte Bunne¹Connor W. Coley²Andreas Krause¹ Regina Barzilay³¹Department of Computer Science, ETH²Department of Chemical Engineering, MIT³Computer Science and Artificial Intelligence Lab, MIT¹{vsomnath, bunnec, krausea}@ethz.ch, ²ccoley@mit.edu, ³regina@csail.mit.edu

Abstract

Retrosynthesis prediction is a fundamental problem in organic synthesis, where the task is to identify precursor molecules that can be used to synthesize a target molecule. Despite recent advancements in neural retrosynthesis algorithms, they are unable to fully recapitulate the strategies employed by chemists and do not generalize well to infrequent reaction types. In this paper, we propose a graph-based approach that capitalizes on the idea that the graph topology of precursor molecules is largely unaltered during the reaction. The model first predicts the set of graph edits transforming the target into incomplete molecules called *synthons*. Next, the model learns to expand synthons into complete molecules by attaching relevant *leaving groups*. Since the model operates at the level of molecular fragments, it avoids full generation, greatly simplifying the underlying architecture and improving its ability to generalize. The model yields 11.7% absolute improvement over state-of-the-art approaches on the USPTO-50k dataset, and a 4% absolute improvement on a rare reaction subset of the same dataset.

1 Introduction

Retrosynthesis prediction, first formalized by E.J. Corey [7], is a fundamental problem in organic synthesis that attempts to identify a series of chemical transformations for synthesizing a target molecule. In the single-step formulation, the task is to identify a set of reactant molecules given a target. The problem is challenging as the space of possible transformations is vast, and requires the skill of experienced chemists. Since the 1960s, retrosynthesis prediction has seen assistance from modern computing techniques [6], with a recent surge in machine learning methods [2, 4, 8, 27].

Existing machine learning methods for retrosynthesis prediction fall into template-based [4, 8, 21] and template-free approaches [2, 27]. Template-based methods match the target molecule against a large set of templates, which are molecular subgraph patterns that highlight changes during a chemical reaction. Despite their interpretability, these methods suffer from poor generalization to new and rare reactions. Template-free methods bypass templates by learning a direct mapping from the SMILES representations [25] of the product to reactants. Despite their greater generalization potential, these methods generate reactant SMILES character by character, failing to utilize the largely conserved substructures in a chemical reaction.

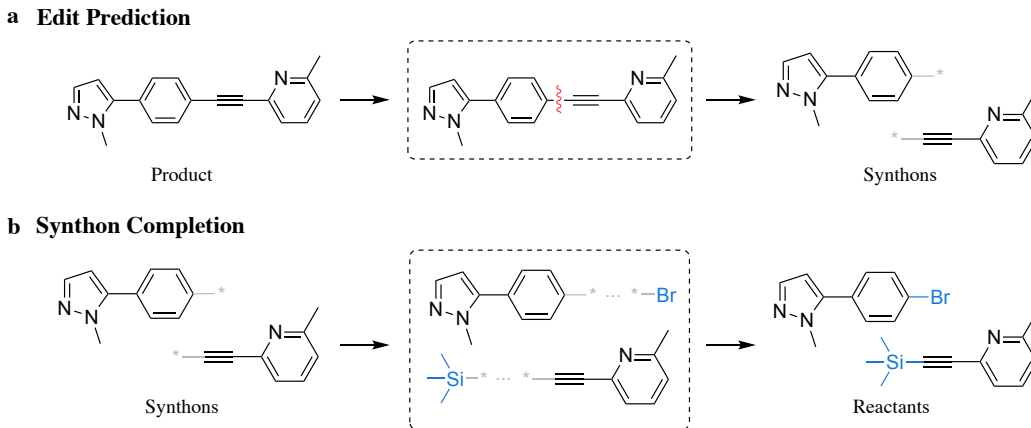


Figure 1: **Overview of Our Approach.** **a. Edit Prediction.** We train a model to learn a distribution over possible graph edits, In this case, the correct edit corresponds to breaking the bond marked in red. Applying this edit produces two synthons. **b. Synthon Completion.** Another model is trained to pick candidate leaving groups (blue) for each synthon from a discrete vocabulary, which are then attached to produce the final reactants.

A chemical reaction satisfies two *fundamental* properties: (i.) the product atoms are always a subset of the reactant atoms¹, and (ii.) the molecular graph topology is largely unaltered from products to reactants. For example, in the standard retrosynthesis dataset, only 6.3% of the atoms in the product undergo any change in connectivity. Our approach is motivated by the hypothesis that utilizing subgraphs within the product to generate reactants can significantly improve the performance and generalization ability of retrosynthesis models.

Our template-free approach called GRAPHRETRO generates reactants in two stages: (i.) deriving intermediate molecules called synthons from the product molecule, and (ii.) expanding synthons into reactants by adding specific functionalities called leaving groups. For deriving synthons, we utilize the rarity of new bond formations to predict a score for existing bonds and atoms instead of each atom pair. This reduces the prediction complexity from $O(N^2)$ to $O(N)$. Furthermore, we incorporate global dependencies into our prediction input by using convolutional layers. For completing synthons into reactants, we select leaving groups from a precomputed vocabulary. The vocabulary is constructed during preprocessing by extracting subgraphs that differ between a synthon and the corresponding reactant, and has a 99.7% coverage on the test set.

We evaluate GRAPHRETRO on the benchmark USPTO-50k dataset and a subset of the same dataset that consists of rare reactions. On the USPTO-50k dataset, GRAPRETRO achieves 64.2% top-1 accuracy without the knowledge of reaction class, outperforming the state-of-the-art method by a margin of 11.7%. On the rare reaction subset, GRAPHRETRO achieves 31.5% top-1 accuracy, with a 4% margin over the state-of-the-art method.

2 Related Work

Retrosynthesis Prediction Existing machine learning methods for retrosynthesis prediction can be divided into template-based and template-free approaches. Templates are either hand-crafted by experts [10, 23], or extracted algorithmically from large databases [3, 16]. Exhaustively applying large template sets is expensive due to the involved subgraph matching procedure. Template-based methods therefore utilize different ways of prioritizing templates, by either learning a conditional distribution over the template set [21], ranking templates based on molecular similarities to precedent reactions [4] or directly modelling the joint distribution of templates and reactants using logic variables [8]. Despite their interpretability, these methods fail to generalize outside their rule set.

Template-free methods [17, 27, 2] bypass templates by learning a direct transformation from products to reactants. Current methods leverage architectures from neural machine translation and use string

¹ignoring impurities

based representation of molecules called SMILES [25]. Linearizing molecules as strings does not utilize the inherently rich chemical structure. In addition, the reactant SMILES are generated from scratch, character by character. Attempts have been made to improve validity by adding a syntax correcter [27] and a mixture model to improve diversity of suggestions [2], but the performance remains worse than [8] on the standard retrosynthesis dataset.

Reaction Center Identification Our work most closely relates to models that predict reaction outcomes based on the reaction center [5, 11]. This center covers a small number of participating atoms involved in the reaction. By learning to rank atom pairs based on their likelihood to be in the reaction center, these models can predict reaction outcomes. In the contemporary, work [22] directly applied this idea to graph-based retrosynthesis. However, their performance falls short of the state-of-the-art performance. The task of identifying the reaction center is related to the step of deriving the synthons in our formulation. Our work departs from [5, 11] as we utilize the property that new bond formations occur rarely ($\sim 0.1\%$) from products to synthons, allowing us to predict a score only for existing bonds and atoms and reduce prediction complexity from $O(N^2)$ to $O(N)$. We further introduce global dependencies into the prediction input by using convolutional layers. This novel architecture yield over 11% improvement over state-of-the-art approaches.

Utilizing Substructures Substructures have been utilized in various tasks from sentence generation by fusing phrases to molecule generation and optimization [12, 13]. Our work is closely related to [13] which uses precomputed substructures as building blocks for property-conditioned molecule generation. However, instead of precomputing, synthons —analogous building blocks for reactants— are indirectly learnt during training.

3 Model Design

Our approach leverages the property that graph topology is largely unaltered from products to reactants. To achieve this, we first derive suitable building blocks from the product called *synthons*, and then complete them into valid reactants by adding specific functionalities called *leaving groups*. These derivations, called *edits*, are characterized by modifications to bonds or hydrogen counts on atoms. We first train a neural network to predict a score for possible edits (Section 3.1). The edit with the highest score is then applied to the product to obtain synthons. Since the number of unique leaving groups are small, we model leaving group selection as a classification problem over a precomputed vocabulary (Section 3.2). To produce candidate reactants, we attach the predicted leaving group to the corresponding synthon through chemically constrained rules. The overall process is outlined in Figure 1. Before describing the two modules, we introduce relevant preliminaries that set the background for the remainder of the paper.

Retrosynthesis Prediction A retrosynthesis pair R is described by a pair of molecular graphs $(\mathcal{G}_p, \mathcal{G}_r)$, where \mathcal{G}_p are the products and \mathcal{G}_r the reactants. A molecular graph is described as $\mathcal{G} = (\mathcal{V}, \mathcal{E})$ with atoms \mathcal{V} as nodes and bonds \mathcal{E} as edges. Prior work has focused on the single product case, while reactants can have multiple connected components, i.e. $\mathcal{G}_r = \{\mathcal{G}_{r_c}\}_{c=1}^C$. Retrosynthesis pairs are *atom-mapped* so that each product atom has a unique corresponding reactant atom. The retrosynthesis task then, is to infer $\{\mathcal{G}_{r_c}\}_{c=1}^C$ given \mathcal{G}_p .

Edits Edits consist of (i.) atom pairs $\{(a_i, a_j)\}$ where the bond type changes from products to reactants, and (ii.) atoms $\{a_i\}$ where the number of hydrogens attached to the atom change from products to reactants. We denote the set of edits by E . Since retrosynthesis pairs in the training set are atom-mapped, edits can be automatically identified by comparing the atoms and atom pairs in the product to their corresponding reactant counterparts.

Synthons and Leaving Groups Applying edits E to the product \mathcal{G}_p results in incomplete molecules called *synthons*. Synthons are analogous to rationales or building blocks, which are expanded into valid reactants by adding specific functionalities called *leaving groups* that are responsible for its reactivity. We denote synthons by \mathcal{G}_s and leaving groups by \mathcal{G}_l . We further assume that synthons and leaving groups have the same number of connected components as the reactants, i.e $\mathcal{G}_s = \{\mathcal{G}_{s_c}\}_{c=1}^C$ and $\mathcal{G}_l = \{\mathcal{G}_{l_c}\}_{c=1}^C$. This assumption holds for 99.97% reactions in the training set.

Formally, our model generates reactants by first predicting the set of edits E that transform \mathcal{G}_p into \mathcal{G}_s , followed by predicting a leaving group \mathcal{G}_{l_e} to attach to each synthon \mathcal{G}_{s_e} . The model is defined as

$$P(\mathcal{G}_r|\mathcal{G}_p) = \sum_{E, \mathcal{G}_l} P(E|\mathcal{G}_p)P(\mathcal{G}_l|\mathcal{G}_p, \mathcal{G}_s), \quad (1)$$

where $\mathcal{G}_s, \mathcal{G}_r$ are deterministic given E, \mathcal{G}_l , and \mathcal{G}_p .

3.1 Edit Prediction

For a given retrosynthesis pair $R = (\mathcal{G}_p, \mathcal{G}_r)$, we predict an edit score only for existing bonds and atoms, instead of every atom pair as in [5, 11]. This choice is motivated by the low frequency ($\sim 0.1\%$) of new bond formations in the training set examples. Coupled with the sparsity of molecular graphs², this reduces the prediction complexity from $O(N^2)$ to $O(N)$ for a product with N atoms. Our edit prediction model has variants tailored to single and multiple edit prediction. Since 95% of the training set consists of single edit examples, the remainder of this section describes the setup for single edit prediction. A detailed description of our multiple edit prediction model can be found in Appendix B.

Each bond (u, v) in \mathcal{G}_p is associated with a label $y_{uvk} \in \{0, 1\}$ indicating whether its bond type k has changed from the products to reactants. Each atom u is associated with a label $y_u \in \{0, 1\}$ indicating a change in hydrogen count. We predict edit scores using representations that are learnt using a graph encoder.

Graph Encoder To obtain atom representations, we use a variant of the *message passing network* (MPN) described in [9]. Each atom u has a feature vector \mathbf{x}_u indicating its atom type, degree and other properties. Each bond (u, v) has a feature vector \mathbf{x}_{uv} indicating its aromaticity, bond type and ring membership. For simplicity, we denote the encoding process by $\text{MPN}(\cdot)$ and describe architectural details in Appendix A. The MPN computes atom representations $\{\mathbf{c}_u | u \in \mathcal{G}\}$ via

$$\{\mathbf{c}_u\} = \text{MPN}(\mathcal{G}, \{\mathbf{x}_u\}, \{\mathbf{x}_{uv}\}_{v \in \mathcal{N}(u)}), \quad (2)$$

where $\mathcal{N}(u)$ denotes the neighbors of atom u . The graph representation $\mathbf{c}_{\mathcal{G}}$ is an aggregation of atom representations, i.e. $\mathbf{c}_{\mathcal{G}} = \sum_{u \in \mathcal{V}} \mathbf{c}_u$. When \mathcal{G} has connected components $\{\mathcal{G}_i\}$, we get a set of graph representations $\{\mathbf{c}_{\mathcal{G}_i}\}$. For a bond (u, v) , we define its representation $\mathbf{c}_{uv} = (\mathbf{c}_u || \mathbf{c}_v)$ as the concatenation of atom representations \mathbf{c}_u and \mathbf{c}_v , where $||$ refers to concatenation.

Using these representations to directly predict edit scores constrains predictions to the neighborhood the messages were aggregated from. We include global dependencies in the prediction input by using convolutional layers, which have been used successfully to extract globally occurring features using locally operating filters [14, 19]. We apply P layers of convolutions to atom and bond representations to obtain embeddings \mathbf{c}_u^P and \mathbf{c}_{uv}^P . These representations are then used to predict atom and bond edit scores using corresponding neural networks,

$$s_u = \mathbf{u}_a^T \tau(\mathbf{W}_a \mathbf{c}_u^P + b) \quad (3)$$

$$s_{uvk} = \mathbf{u}_k^T \tau(\mathbf{W}_k \mathbf{c}_{uv}^P + b_k), \quad (4)$$

where $\tau(\cdot)$ is the ReLU activation function.

Training We train by minimizing the cross-entropy loss over possible bond and atom edits

$$\mathcal{L}_e = - \sum_{(\mathcal{G}_p, E)} \left(\sum_{((u,v),k) \in E} y_{uvk} \log(s_{uvk}) + \sum_{u \in E} y_u \log(s_u) \right). \quad (5)$$

The cross-entropy loss enforces the model to learn a distribution over possible edits instead of reasoning about each edit independently, as with the binary cross entropy loss used in [11, 5].

² $M \sim N$, for a molecule with N atoms and M bonds

3.2 Synthon Completion

Synthons are completed into valid reactants by adding specific functionalities called *leaving groups*. This involves two complementary tasks: (i.) selecting the appropriate leaving group, and (ii.) attaching the leaving group to the synthon. As ground truth leaving groups are not directly provided, we extract the leaving groups and construct a vocabulary \mathcal{X} of unique leaving groups during preprocessing. The vocabulary has a limited size ($|\mathcal{X}| = 170$ for a standard dataset with 50,000 examples). We thus formulate leaving group selection as a classification problem over \mathcal{X} .

Vocabulary Construction Before constructing the vocabulary, we align connected components of synthon and reactant graphs by comparing atom mapping overlaps. Using aligned pairs $\mathcal{G}_{s_c} = (\mathcal{V}_{s_c}, \mathcal{E}_{s_c})$ and $\mathcal{G}_{r_c} = (\mathcal{V}_{r_c}, \mathcal{E}_{r_c})$ as input, the leaving group vocabulary \mathcal{X} is constructed by extracting subgraphs $\mathcal{G}_{l_c} = (\mathcal{V}_{l_c}, \mathcal{E}_{l_c})$ such that $\mathcal{V}_{l_c} = \mathcal{V}_{r_c} \setminus \mathcal{V}_{s_c}$. Atoms $\{a_i\}$ in the leaving groups that attach to synthons are marked with a special symbol. We also add three tokens to \mathcal{X} namely START, which indicates the start of synthon completion, END, which indicates that there is no leaving group to add and PAD, which is used to handle variable numbers of synthon components in a minibatch.

Leaving Group Selection Treating each $x_i \in \mathcal{X}$ as a molecular subgraph, we learn representations \mathbf{e}_{x_i} using the MPN(\cdot). We also use the same MPN(\cdot) to learn the product graph representation $\mathbf{c}_{\mathcal{G}_p}$ and synthon representations $\{\mathbf{c}_{\mathcal{G}_{s_c}}\}_{c=1}^C$, where C is the number of connected components. For each step $c \leq C$, we compute leaving group probabilities by combining the product representation $\mathbf{c}_{\mathcal{G}_p}$, the synthon component representation $\mathbf{c}_{\mathcal{G}_{s_c}}$ and the representation of leaving group in the previous stage $\mathbf{e}_{l_{c-1}}$ via a single layer neural network and softmax function

$$\hat{q}_{l_c} = \text{softmax}(\mathbf{U}\tau(\mathbf{W}_1\mathbf{c}_{\mathcal{G}_p} + \mathbf{W}_2\mathbf{c}_{\mathcal{G}_{s_c}} + \mathbf{W}_3\mathbf{e}_{l_{c-1}})), \quad (6)$$

where \hat{q}_{l_c} is distribution learnt over \mathcal{X} . Using the representation of the previous leaving group $\mathbf{e}_{l_{c-1}}$ allows the model to understand *combinations* of leaving groups that generate the desired product from the reactants. We also include the product representation $\mathbf{c}_{\mathcal{G}_p}$ as the synthon graphs are derived from the product graph.

Training For step c , given the one hot encoding of the true leaving group q_{l_c} , we minimize the cross-entropy loss

$$\mathcal{L}_s = \sum_{c=1}^C \mathcal{L}(\hat{q}_{l_c}, q_{l_c}). \quad (7)$$

Training utilizes teacher-forcing [26] so that the model makes predictions given correct histories. During inference, at every step, we use the representation of leaving group from the previous step with the highest predicted probability.

Leaving Group Attachment Attaching leaving groups to synthons is a deterministic process and not learnt during training. The task involves identification of the type of bonds to add between attaching atoms in the leaving group (marked during vocabulary construction), and the atom(s) participating in the edit. These bonds can be inferred by applying the *valency* constraint, which determines the maximum number of neighbors for each atom. Given synthons and leaving groups, the attachment process has a 100% accuracy. The detailed procedure is described in Appendix C.

3.3 Overall Training and Inference

The two modules can either be trained separately (referred to as *separate*) or jointly by sharing the encoder (*shared*). Sharing the encoder between edit prediction and synthon completion modules allows us to train the model end-to-end. The shared training minimizes the loss $\mathcal{L} = \lambda_e\mathcal{L}_e + \lambda_s\mathcal{L}_s$, where λ_e and λ_s weigh the influence of each term on the final loss.

Inference is performed using beam search with a log-likelihood scoring function. For a beam width n , we select n edits with highest scores and apply them to the product to obtain n synthons, where each synthon can consist of multiple connected components. The synthons form the nodes for beam search.

Each node maintains a cumulative score by aggregating the log-likelihoods of the edit and predicted leaving groups. Leaving group inference starts with a connected component for each synthon, and selects n leaving groups with highest log-likelihoods. From the n^2 possibilities, we select n nodes with the highest cumulative scores. This process is repeated until all nodes have a leaving group predicted for each synthon component.

4 Experiments

Evaluating retrosynthesis models is challenging as multiple sets of reactants can be generated from the same product through a combination of different edits and/or leaving groups. To deal with this, previous works [4, 8] evaluate the ability of the model to recover retrosynthetic strategies recorded in the dataset. However, this evaluation does not directly measure the generalization to infrequent reactions. Chen et al. [2] further evaluate on a rare reaction subset of the standard dataset, and note that model performance drops by almost 25% on such reactions compared to the overall performance.

Our evaluation quantifies two scenarios, (i.) overall performance on the standard dataset, and (ii.) generalization ability via rare reaction performance. We also evaluate the performance of the edit prediction and synthon completion modules to gain more insight into the working of our model.

Data We use the benchmark dataset USPTO-50k [20] for all our experiments. The dataset contains 50,000 atom-mapped reactions across 10 reaction classes. Following prior work [4, 8], we divide the dataset randomly in an 80:10:10 split for training, validation and testing. For evaluating generalization, we use a subset of rare reactions from the same dataset, consisting of 512 reactions. Details on the construction of this subset can be found in Appendix D.3.

Evaluation We use the top- n accuracy ($n = 1, 3, 5, 10, 50$) as our evaluation metric, defined as the fraction of examples where the recorded reactants are suggested by the model with rank $\leq n$. Following prior work [4, 27, 8], we compute the accuracy by comparing the canonical SMILES of predicted reactants to the ground truth. Atom-mapping is excluded from this comparison, but stereochemistry, which describes the relative orientation of atoms in the molecule, is retained. The evaluation is carried out for both cases where the reaction class is known or unknown.

Baselines For evaluating overall performance, we compare GRAPHRETRO to six baselines—three template-based and three template-free models. For evaluating rare reaction performance, we compare only against GLN which is the state-of-the-art method. The baseline methods include:

Template-Based: RETROSIM [4] ranks templates for a given target molecule by computing molecular similarities to precedent reactions. NEURALSVM [21] trains a model to rank templates given a target molecule. The state-of-the-art method GLN [8] models the joint distribution of templates and reactants in a hierarchical fashion using logic variables.

Template-Free: SCROP [27] and LV-TRANSFORMER [2] use the Transformer architecture [24] to output reactant SMILES given a product SMILES. To improve the validity of their suggestions, SCROP include a second Transformer that functions as a syntax corrector. LV-TRANSFORMER uses a latent variable mixture model to improve diversity of suggestions. G2Gs [22] is a contemporary graph-based retrosynthesis prediction approach that first identifies synthons and expands synthons into valid reactants using a variational graph translation module.

4.1 Overall Performance

Results As shown in Table 1, when the reaction class is unknown, GRAPHRETRO’s *shared* and *separate* configurations outperform GLN by 11.7% and 11.3% in top-1 accuracy, achieving state-of-the-art performance. Similar improvements are achieved for larger n , with ~84% of the true precursors in the top-5 choices. Barring GLN, GRAPHRETRO’s top-5 and top-10 accuracies are comparable to the top-50 accuracies of template-based methods, especially in the unknown reaction class setting. When the reaction class is known, RETROSIM and GLN restrict template sets corresponding to the reaction class, thus improving performance. Both of our model configurations outperform the other methods till $n = 5$.

Table 1: **Overall Performance**³. (sh) and (se) denote *shared* and *separate* training.

Model	Top- n Accuracy (%)										
	$n =$	Reaction class known					Reaction class unknown				
		1	3	5	10	50	1	3	5	10	50
Template-Based											
RETROSIM [4]	52.9	73.8	81.2	88.1	92.9	37.3	54.7	63.3	74.1	85.3	
NEURALSVM [21]	55.3	76.0	81.4	85.1	86.9	44.4	65.3	72.4	78.9	83.1	
GLN [8]	64.2	79.1	85.2	90.0	93.2	52.5	69.0	75.6	83.7	92.4	
Template-Free											
SCROP [27]	59.0	74.8	78.1	81.1	-	43.7	60.0	65.2	68.7	-	
LV-TRANSFORMER [2]	-	-	-	-	-	40.5	65.1	72.8	79.4	-	
G2Gs [22]	61.0	81.3	86.0	88.7	-	48.9	67.6	72.5	75.5	-	
GRAPHRETRO (sh)	67.2	81.7	84.6	87.0	87.2	64.2	78.6	81.4	83.1	84.1	
GRAPHRETRO (se)	67.8	82.7	85.3	87.0	87.9	63.8	80.5	84.1	85.9	87.2	

Parameter Sharing The benefits of sharing the encoder are indicated by comparable performances of the *shared* and *separate* configurations. In the *shared* configuration, the synthon completion module is trained only on the subset of leaving groups that correspond to single-edit examples. In the *separate* configuration, the synthon completion module is trained on all leaving groups. For reference, the *separate* configuration with the synthon completion module trained on the same subset as the *shared* configuration achieves a 62.1% top-1 accuracy in the unknown reaction class setting.

4.2 Rare Reactions

From Table 2, we note that for rare reactions, the performance of all methods drops significantly. Despite the low template frequency, GLN’s performance can be explained by its hierarchical model design that first ranks precomputed reaction centers, allowing the model to focus on relevant parts of the molecule. Instead of precomputing centers, our model learns to identify the correct edit (and consequently reaction centers), thus improving the top-1 accuracy by 4% over GLN.

Table 2: **Rare Reaction Performance**. (sh) and (se) denote *shared* and *separate* configurations.

Model	Top- n Accuracy (%)				
	1	3	5	10	50
GLN	27.5	35.7	39.3	46.1	55.9
GRAPHRETRO (sh)	31.5	40.2	43.6	45.3	48.6
GRAPHRETRO (se)	30.1	40.2	45.1	48.2	52.2

4.3 Individual Module Performance

To gain more insight into the working of GRAPHRETRO, we evaluate the top- n accuracy ($n = 1, 2, 3, 5$) of edit prediction and synthon completion modules, with results shown in Table 3.

Edit Prediction For the edit prediction module, we compare the true edits to top- n edits predicted by the model. When the reaction class is known, edits are predicted with a top-5 accuracy of 94%, close to its theoretical upper bound of 95.1% (% of single-edit examples). When the reaction class is unknown, the model achieves a top-1 accuracy of almost 90%. Identifying the correct edit is necessary for generating the true reactants.

Synthon Completion For the synthon completion module, we first apply the true edits to obtain synthons, and compare the true leaving groups to top- n leaving groups predicted by the model. The

³results for NEURALSVM are taken from [8], for other baselines, we use their reported results

synthon completion module is able to identify ~ 97% (close to its upper bound of 99.7%) of the true leaving groups in its top-5 choices.

Table 3: **Performance Study** of edit prediction and synthon completion modules

Setting	Top- n Accuracy (%)								
	$n =$	Reaction class known				Reaction class unknown			
		1	2	3	5	1	2	3	5
Edit Prediction		91.4	93.1	93.6	94.0	89.8	92.1	92.6	93.2
Synthon Completion		77.1	89.2	93.6	96.9	73.9	87.0	92.6	96.6

4.4 Example Predictions

In Figure 2, we visualize the model predictions and the ground truth for three cases. Figure 2a shows an example where the model identifies both the edits and leaving groups correctly. In Figure 2b, the correct edit is identified but the predicted leaving groups are incorrect. We hypothesize this is due to the fact that in the training set, leaving groups attaching to the carbonyl carbon (C=O) are small (e.g. -OH, -NH₂, halides). The true leaving group in this example, however, is large. The model is unable to reason about this and predicts the small leaving group -I. In Figure 2c, the model identifies the edit and consequently the leaving group incorrectly. This highlights a limitation of our model. If the edit is predicted incorrectly, the model cannot suggest the true precursors.

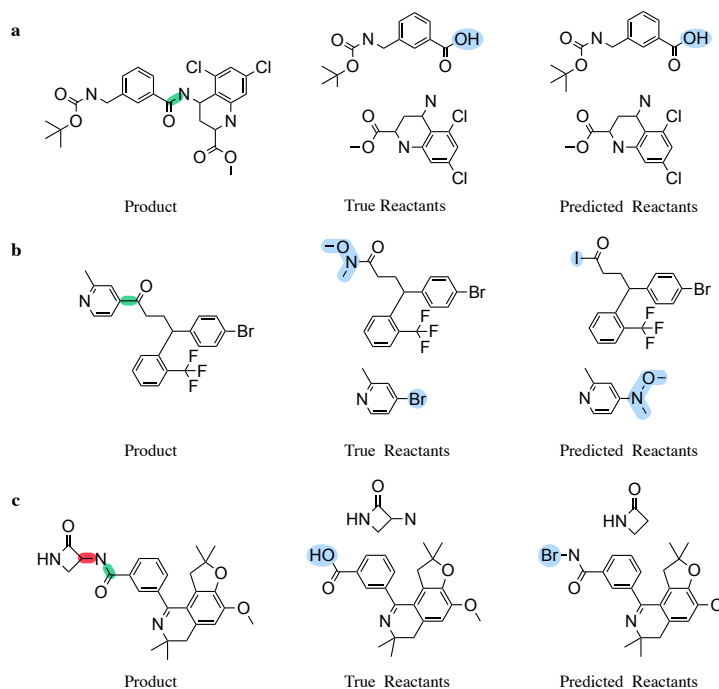


Figure 2: **Example Predictions.** The true edit and incorrect edit (if any) are highlighted in green and red respectively. The true and predicted leaving groups are highlighted in blue. **a.** Correctly predicted example by the model. **b.** Correctly predicted edit but incorrectly predicted leaving groups. **c.** Incorrectly predicted edit and leaving group.

5 Conclusion

Previous methods for single-step retrosynthesis either restrict prediction to a template set, are insensitive to molecular graph structure or generate molecules from scratch. We address these

shortcomings by introducing a graph-based template-free model inspired by a chemist's workflow. Given a target molecule, we first identify synthetic building blocks (*synthons*) which are then realized into valid reactants, thus avoiding molecule generation from scratch. Our model outperforms previous methods by significant margins on the benchmark dataset and a rare reaction subset of the same dataset. Future work aims to extend the model to realize a single reactant from multiple synthons, and develop pretraining strategies specific to reaction chemistry to improve rare reaction performance.

Broader Impact

Our research advances template-free models for computer-aided retrosynthesis by incorporating a chemist's workflow into the design. In addition to achieving improved accuracy, our formulation has the potential to make retrosynthetic workflows more flexible and interactive by allowing users to supply their own edits and not use the edit prediction module for inference. These tools are intended to reduce the time investment required to physically produce computationally-designed molecules (e.g. drug candidates) and make the process of molecular discovery cheaper and faster. Long-term, they may enable the automation of routine chemistry using common organic transformations, which would encourage a reallocation of human chemist creativity to more complex synthesis tasks (e.g. the synthesis of more complex molecules, stereoselectivity, discovery of new reaction types) for which models cannot make accurate predictions.

References

- [1] J. Bradshaw, M. J. Kusner, B. Paige, M. H. S. Segler, and J. M. Hernández-Lobato. A Generative Model For Electron Paths. In *International Conference on Learning Representations (ICLR)*, 2019.
- [2] B. Chen, T. Shen, T. S. Jaakkola, and R. Barzilay. Learning to Make Generalizable and Diverse Predictions for Retrosynthesis. In Submission, 2019.
- [3] C. W. Coley, R. Barzilay, T. S. Jaakkola, W. H. Green, and K. F. Jensen. Prediction of Organic Reaction Outcomes Using Machine Learning. In *ACS Central Science*. ACS Publications, 2017.
- [4] C. W. Coley, L. Rogers, W. H. Green, and K. F. Jensen. Computer-Assisted Retrosynthesis Based on Molecular Similarity. *ACS Central Science*, 3, 2017.
- [5] C. W. Coley, W. Jin, L. Rogers, T. F. Jamison, T. S. Jaakkola, W. H. Green, R. Barzilay, and K. F. Jensen. A graph-convolutional neural network model for the prediction of chemical reactivity. *Chemical Science*, 10, 2019.
- [6] E. Corey and W. T. Wipke. Computer-assisted design of complex organic syntheses. *Science*, 166(3902):178–192, 1969.
- [7] E. J. Corey. The Logic of Chemical Synthesis: Multistep Synthesis of Complex Carbogenic Molecules (Nobel Lecture). *Angewandte Chemie International Edition*, 30, 1991.
- [8] H. Dai, C. Li, C. Coley, B. Dai, and L. Song. Retrosynthesis Prediction with Conditional Graph Logic Network. In *Advances in Neural Information Processing Systems (NeurIPS)*, volume 32, 2019.
- [9] J. Gilmer, S. S. Schoenholz, P. F. Riley, O. Vinyals, and G. E. Dahl. Neural Message Passing for Quantum Chemistry. In *International Conference on Machine Learning (ICML)*, volume 70, 2017.
- [10] M. Hartenfeller, M. Eberle, P. Meier, C. Nieto-Oberhuber, K.-H. Altmann, G. Schneider, E. Jacoby, and S. Renner. A Collection of Robust Organic Synthesis Reactions for In Silico Molecule Design. In *Journal of Chemical Information and Modeling*, volume 51. ACS Publications, 2011.
- [11] W. Jin, C. Coley, R. Barzilay, and T. Jaakkola. Predicting Organic Reaction Outcomes with Weisfeiler-Lehman Network. In *Advances in Neural Information Processing Systems (NeurIPS)*, volume 30, 2017.
- [12] W. Jin, R. Barzilay, and T. Jaakkola. Junction Tree Variational Autoencoder for Molecular Graph Generation. In *International Conference on Machine Learning (ICML)*, volume 32, 2018.

- [13] W. Jin, R. Barzilay, and T. Jaakkola. Composing Molecules with Multiple Property Constraints. In *International Conference on Machine Learning (ICML)*, 2020.
- [14] A. Krizhevsky, I. Sutskever, and G. E. Hinton. Imagenet classification with deep convolutional neural networks. In *Advances in neural information processing systems*, pages 1097–1105, 2012.
- [15] G. Landrum. RDKit: Open-Source Cheminformatics Software. 2016.
- [16] J. Law, Z. Zsoldos, A. Simon, D. Reid, Y. Liu, S. Y. Khew, A. P. Johnson, S. Major, R. A. Wade, and H. Y. Ando. Route Designer: A Retrosynthetic Analysis Tool Utilizing Automated Retrosynthetic Rule Generation. *Journal of Chemical Information and Modeling*, 49, 2009.
- [17] B. Liu, B. Ramsundar, P. Kawthekar, J. Shi, J. Gomes, Q. Luu Nguyen, S. Ho, J. Sloane, P. Wender, and V. Pande. Retrosynthetic Reaction Prediction Using Neural Sequence-to-Sequence Models. In *ACS Central Science*, volume 3. ACS Publications, 2017.
- [18] A. Paszke, S. Gross, F. Massa, A. Lerer, J. Bradbury, G. Chanan, T. Killeen, Z. Lin, N. Gimelshein, L. Antiga, A. Desmaison, A. Kopf, E. Yang, Z. DeVito, M. Raison, A. Tejani, S. Chilamkurthy, B. Steiner, L. Fang, J. Bai, and S. Chintala. PyTorch: An Imperative Style, High-Performance Deep Learning Library. In *Advances in Neural Information Processing Systems (NeurIPS)*, volume 32. 2019.
- [19] W. W. Qian, N. T. Russell, C. L. W. Simons, Y. Luo, M. D. Burke, and J. Peng. Integrating Deep Neural Networks and Symbolic Inference for Organic Reactivity Prediction. In Submission, 2020.
- [20] N. Schneider, N. Stiefl, and G. A. Landrum. What’s What: The (Nearly) Definitive Guide to Reaction Role Assignment. In *Journal of Chemical Information and Modeling*, volume 56. ACS Publications, 2016.
- [21] M. H. Segler and M. P. Waller. Neural-Symbolic Machine Learning for Retrosynthesis and Reaction Prediction. *Chemistry—A European Journal*, 23, 2017.
- [22] C. Shi, M. Xu, H. Guo, M. Zhang, and J. Tang. A graph to graphs framework for retrosynthesis prediction, 2020.
- [23] S. Szymkuć, E. P. Gajewska, T. Klucznik, K. Molga, P. Dittwald, M. Startek, M. Bajczyk, and B. A. Grzybowski. Computer-assisted synthetic planning: The end of the beginning. *Angewandte Chemie International Edition*, 55(20):5904–5937, 2016.
- [24] A. Vaswani, N. Shazeer, N. Parmar, J. Uszkoreit, L. Jones, A. N. Gomez, Ł. Kaiser, and I. Polosukhin. Attention is All You Need. In *Advances in Neural Information Processing Systems (NeurIPS)*, volume 30, 2017.
- [25] D. Weininger. SMILES, a Chemical Language and Information System. *Journal of Chemical Information and Computer Sciences*, 28, 1988.
- [26] R. J. Williams and D. Zipser. A Learning Algorithm for Continually Running Fully Recurrent Neural Networks. In *Neural Computation*, volume 1. MIT Press, 1989.
- [27] S. Zheng, J. Rao, Z. Zhang, J. Xu, and Y. Yang. Predicting Retrosynthetic Reactions using Self-Corrected Transformer Neural Networks. In *Journal of Chemical Information and Modeling*. ACS Publications, 2019.

A Message Passing Network

At message passing step t , each bond $(u, v) \in \mathcal{E}$ is associated with two messages $\mathbf{m}_{uv}^{(t)}$ and $\mathbf{m}_{vu}^{(t)}$. Message $\mathbf{m}_{uv}^{(t)}$ is updated using:

$$\mathbf{m}_{uv}^{(t+1)} = \text{GRU}\left(\mathbf{x}_u, \mathbf{x}_{uv}, \{\mathbf{m}_{wu}^{(t)}\}_{w \in N(u) \setminus v}\right) \quad (8)$$

where GRU denotes the Gated Recurrent Unit, adapted for message passing [12]:

$$\mathbf{s}_{uv} = \sum_{k \in N(u) \setminus v} \mathbf{m}_{ku}^{(t)} \quad (9)$$

$$\mathbf{z}_{uv} = \sigma(\mathbf{W}_z [\mathbf{x}_u, \mathbf{x}_{uv}, \mathbf{s}_{uv}] + b_z) \quad (10)$$

$$\mathbf{r}_{ku} = \sigma(\mathbf{W}_r [\mathbf{x}_u, \mathbf{x}_{uv}, \mathbf{m}_{ku}^{(t)}] + b_r) \quad (11)$$

$$\tilde{\mathbf{r}}_{uv} = \sum_{k \in N(u) \setminus v} \mathbf{r}_{ku} \odot \mathbf{m}_{ku}^{(t)} \quad (12)$$

$$\tilde{\mathbf{m}}_{uv} = \tanh(\mathbf{W} [\mathbf{x}_u, \mathbf{x}_{uv}] + \mathbf{U} \tilde{\mathbf{r}}_{uv} + b) \quad (13)$$

$$\mathbf{m}_{uv}^{(t+1)} = (1 - \mathbf{z}_{uv}) \odot \mathbf{s}_{uv} + \mathbf{z}_{uv} \odot \tilde{\mathbf{m}}_{uv} \quad (14)$$

After T steps of iteration, we aggregate the messages with a neural network $g(\cdot)$ to derive the representation for each atom:

$$\mathbf{c}_u = g\left(\mathbf{x}_u, \sum_{k \in N(u)} \mathbf{m}_{vu}^{(T)}\right) \quad (15)$$

B Multiple Edit Prediction

We propose an autoregressive model for multiple edit prediction that allows us to represent arbitrary length edit sets. The model makes no assumption on the connectivity of the reaction centers or the electron flow topology, addressing the drawbacks mentioned in [1, 11].

Each edit step t uses the intermediate graph $\mathcal{G}_s^{(t)}$ as input, obtained by applying the edits until t to \mathcal{G}_p . Atom and bond labels are now indexed by the edit step, and a new termination symbol $y_d^{(t)}$ is introduced such that $\sum_{(u,v),k} y_{uvk}^{(t)} + \sum_u y_u^{(t)} + y_d^{(t)} = 1$. The number of atoms remain unchanged during edit prediction, allowing us to associate a hidden state $\mathbf{h}_u^{(t)}$ with every atom u . Given representations $\mathbf{c}_u^{(t)}$ returned by the MPN(\cdot) for $\mathcal{G}_s^{(t)}$, we update the atom hidden states as

$$\mathbf{h}_u^{(t)} = \tau\left(\mathbf{W}_h \mathbf{h}_u^{(t-1)} + \mathbf{W}_c \mathbf{c}_u^{(t)} + b\right) \quad (16)$$

The bond hidden state $\mathbf{h}_{uv}^{(t)} = (\mathbf{h}_u^{(t)} || \mathbf{h}_v^{(t)})$ is defined similar to the single edit case. We also compute the termination score using a molecule hidden state $\mathbf{h}_m^{(t)} = \sum_{u \in \mathcal{G}_s^{(t)}} \mathbf{h}_u^{(t)}$. The edit logits are predicted by passing these hidden states through corresponding neural networks:

$$s_{uvk}^{(t)} = \mathbf{u}_k^T \tau\left(\mathbf{W}_k \mathbf{h}_{uv}^{(t)} + b_k\right) \quad (17)$$

$$s_u^{(t)} = \mathbf{u}_a^T \tau\left(\mathbf{W}_a \mathbf{h}_u^{(t)} + b_a\right) \quad (18)$$

$$s_d^{(t)} = \mathbf{u}_d^T \tau\left(\mathbf{W}_d \mathbf{h}_m^{(t)} + b_d\right) \quad (19)$$

Training Training minimizes the cross-entropy loss over possible edits, aggregated over edit steps

$$\mathcal{L}_e(\mathcal{T}_e) = - \sum_{(\mathcal{G}_p, E) \in \mathcal{T}_e} \sum_{t=1}^{|E|} \left(\sum_{(j,k) \in E[t]} y_{uvk}^{(t)} \log(s_{uvk}^{(t)}) + \sum_{u \in E[t]} y_u^{(t)} \log(s_u^{(t)}) + y_d^{(t)} \log(s_d^{(t)}) \right) \quad (20)$$

Training utilizes *teacher-forcing* so that the model makes predictions given correct histories.

C Leaving Group Attachment

Attaching atoms in the leaving groups were marked during vocabulary construction. The number of such atoms are used to divide leaving groups into single and multiple attachment categories. The single attachment leaving groups are further divided into single and double bond attachments depending on the *valency* of the attaching atom. By default, for leaving groups in the multiple attachments category, a single bond is added between attaching atom(s) on the synthon and leaving groups. For multiple attachment leaving groups with a combination of single and double bonds, the attachment is hardcoded. A single edit can result in a maximum of two attaching atoms for the synthon(s). For the case where the model predicts a leaving group with a single attachment, and the predicted edit results in a synthon with two attaching atoms, we attach to the first atom. For the opposite case where we have multiple attaching atoms on the leaving group and a single attaching atom for the synthon, atoms on the leaving group are attached through respective bonds. The former case represents incorrect model predictions, and is not observed as ground truth.

D Experimental Details

Our model is implemented in PyTorch [18]. We also use the open-source software RDKit [15] to process molecules for our training set, for attaching leaving groups to synthons and generating reactant SMILES.

D.1 Input Features

Atom Features We use the following atom features:

- One hot encoding of the atom symbol (65)
- One hot encoding of the degree of the atom (10)
- Explicit valency of the atom (6)
- Implicit valency of the atom (6)
- Whether the atom is part of an aromatic ring (1)

Bond Features We use the following bond features:

- One hot encoding of bond type (4)
- Whether the bond is conjugated (1)
- Whether bond is part of ring (1)

D.2 Retrosynthesis Benchmarks

The hidden layer dimension of the GRU based Message Passing Network is set to 300. We run $T = 10$ iterations of message passing in the encoder. All models are trained with the Adam optimizer and an initial learning rate of 0.001. Gradients are clipped to have a maximum norm of 20.0.

Edit Prediction The global dependency module comprises three convolutional layers with 600, 300 and 150 filters respectively, and a kernel size of 5. The atom and bond edits scoring network has a hidden layer dimension of 300. The model is trained for 100 epochs, and the learning rate is reduced by a factor of 0.9 when a plateau, as measured by the accuracy of predicted edits on the validation set, is observed. The edit prediction model has 2M parameters.

Synthon Completion The embedding dimension of leaving groups is set to 200, and graph representations are projected to the embedding dimension with a learnable projection matrix. The classifier over leaving groups also has a hidden layer dimension of 300, and a dropout probability of 0.2. The synthon completion model has 0.8M parameters.

Shared Encoder Model Trainable parameters of the associated edit prediction and synthon completion modules have the same dimensions as above. We set λ_e to 1.0 and λ_s to 2.0. The model is trained for 100 epochs, and the learning rate is reduced by a factor of 0.9 when a plateau, as measured by the accuracy of predicted edits and leaving groups on the validation set, is observed. The shared encoder model has 2.3M parameters.

D.3 Rare Reactions

To prepare the rare reaction subset of USPTO-50k, we first extract templates from the USPTO-50k training set using the template extraction algorithm in [3]. For this work, we assume a rare template is one which occurs in the training set *atmost* 10 times. Applying this definition to extracted templates results in a rare reaction dataset with 3889 training, 504 development and 512 test reactions.